

Multiresonant forcing of the complex Ginzburg-Landau equation: Pattern selection

Jessica M. Conway and Hermann Riecke

Engineering Sciences and Applied Mathematics, Northwestern University, Evanston, Illinois 60208, USA

(Received 6 June 2007; revised manuscript received 10 September 2007; published 9 November 2007)

We study spatial patterns excited by resonant, multifrequency forcing of systems near a Hopf bifurcation to spatially homogeneous oscillations. Our third-order, weakly nonlinear analysis shows that for small amplitudes only stripe patterns or hexagons (up *and* down) are linearly stable; for larger amplitudes rectangles and super-hexagons may become stable. Numerical simulations show, however, that in the latter regime the third-order analysis is insufficient: superhexagons are unstable. Instead large-amplitude hexagons can arise and be bistable with the weakly nonlinear hexagons.

DOI: [10.1103/PhysRevE.76.057202](https://doi.org/10.1103/PhysRevE.76.057202)

PACS number(s): 82.40.Ck, 47.54.-r, 52.35.Mw, 42.65.Yj

The variety of patterns and planforms that have been observed in surface waves on vertically vibrated fluid surfaces (Faraday waves) is remarkable [1]. As elucidated in various theoretical investigations [2] this extreme variability is a result of the fact that the wave form of the vibration's forcing function allows for a detailed tuning of various aspects of the interaction between different plane-wave modes, which can stabilize complex patterns like superlattice patterns and quasipatterns. Motivated by this richness of patterns we are investigating here the effect of time-periodic forcing with different wave forms on systems undergoing a Hopf bifurcation to spatially homogeneous oscillations.

In order to describe a forced Hopf bifurcation within a weakly nonlinear framework the forcing must be sufficiently weak. It nevertheless has a particularly strong effect on the system if it includes frequencies that are close to one or more of the low-order resonances of the system, i.e., if its spectrum contains frequencies close to the Hopf frequency ω_h itself (1:1-forcing), close to $2\omega_h$ (2:1-forcing), or close to $3\omega_h$ (3:1-forcing) [3]. These strong resonances lead to additional terms in the weakly nonlinear description and qualitatively affect the system [4]. To wit, in the weakly nonlinear regime the complex oscillation amplitude A satisfies a complex Ginzburg-Landau equation of the form

$$\frac{dA}{dt} = (\mu + i\nu)A + (1 + i\beta)\Delta A - (1 + i\alpha)A|A|^2 + \gamma\bar{A} + \eta\bar{A}^2 + \zeta. \quad (1)$$

Note that γ can be chosen real without loss of generality as the argument Φ of γ can be absorbed into A through a transformation $A \rightarrow Ae^{i\Phi/2}$. The forcing terms ζ , $\gamma\bar{A}$, and $\eta\bar{A}^2$ represent the effect of forcing the system at the frequencies ω , 2ω , and 3ω , respectively, with $\omega = \omega_h + \frac{\nu}{2}$. The forcing is assumed to be small with $\gamma = O(\mu) = O(\eta^2) = O(\zeta^{2/3})$. The parameter μ expresses the distance from the Hopf bifurcation, which is shifted by a term of $O(|\eta|^2)$ compared to the unforced case. Here we will focus on $\zeta=0$. To include the forcing near the 1:1-resonance one can eliminate the inhomogeneous term ζ by using the fixed-point solution A_0 , which satisfies $\zeta = -(\mu + i\nu)A_0 + (1 + i\alpha)A_0|A_0|^2 - \gamma\bar{A}_0 - \eta\bar{A}_0^2$, instead of ζ as a control parameter [5]. This shift introduces the additional nonlinear terms A^2 and $|A|^2$.

As is apparent from Eq. (1), the forced Hopf bifurcation is described by an equation that is very similar to a two-component reaction-diffusion equation. The only and significant difference is the term involving β which characterizes the dispersion of unforced traveling wave solutions, which would be absent in the reaction-diffusion context. It plays, however, an essential role in exciting patterns with a characteristic wave number [6] and cannot be omitted. Pattern selection in a general two-component reaction-diffusion system has been studied in detail by Judd and Silber [7], who find that in principle not only stripe and hexagon patterns can be stable in such systems, but also supersquare and superhexagon patterns. They show that despite the large number of parameters characterizing these systems surprisingly few, very special combinations of the parameters enter the equations determining the pattern selection.

Amplitude equations. In this Brief Report we will stay below the Hopf bifurcation taking $\mu < 0$. Thus, as in Faraday systems, in the absence of forcing, no oscillations arise. To investigate the weakly nonlinear stable standing wave patterns possible in Eq. (1) we derive amplitude equations for spatially periodic planforms. The linear stability of the state $A=0$ is easily obtained by splitting the equation and the amplitude A into real and imaginary parts ($A \equiv A_r + iA_i$). The usual Fourier ansatz $A_{r,i} \propto e^{ikx}$ yields then the neutral stability curve $\gamma_n(k)$ with the basic state being unstable for $\gamma > \gamma_n(k)$. The minimum $\gamma_c(k)$ of the neutral curve is found to be at $k_c^2 = (\mu + \nu\beta)/(1 + \beta^2)$, $\gamma_c^2 = (\nu - \mu\beta)^2/(1 + \beta^2)$. Since $\mu < 0$, the condition $k_c^2 > 0$ implies that spatial patterns arise only if the detuning of the forcing relative to the Hopf frequency is such that waves with nonzero k are closer to resonance than homogeneous oscillations with $k=0$ [6]. A typical neutral curve is illustrated in Fig. 1 for $\mu = -1$, $\nu = 4$, $\beta = 3$, and $\zeta = 0$. The weakly nonlinear analysis presented in this Brief Report is valid for values of γ near γ_c . The range of validity is restricted by $\gamma_n(k=0)$ where spatially homogeneous oscillations are excited by the forcing, which interacts with the standing-wave modes with wave number k_c .

To determine the stability of the various planforms we first determine the amplitude equations for rectangle patterns, which are comprised of two modes separated by an angle θ in Fourier space. We expand (A_r, A_i) as

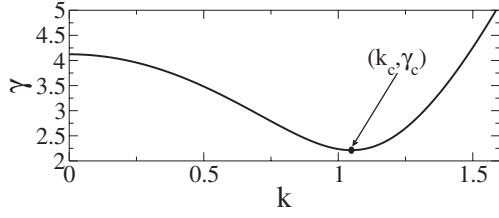


FIG. 1. Neutral stability curve for Eq. (1) with $\mu=-1$, $\beta=3$, $\nu=4$, and $\zeta=0$, resulting in $k_c=\sqrt{11/10}$ and $\gamma_c=7/\sqrt{10}$.

$$\begin{pmatrix} A_r \\ A_i \end{pmatrix} = \epsilon \sum_{j=1,\theta} Z_j(T) e^{ik_j \cdot r} \begin{pmatrix} v_1 \\ v_2 \end{pmatrix} + \text{c.c.} + O(\epsilon^2), \quad (2)$$

where $0 < \epsilon \ll 1$ and the complex amplitudes $Z_1(T)$ and $Z_\theta(T)$ depend on the slow time $T = \epsilon^2 t$. The wave vectors are given by $\mathbf{k}_1 = (k_c, 0)$ and $\mathbf{k}_\theta = [k_c \cos(\theta), k_c \sin(\theta)]$. We also expand γ as $\gamma = \gamma_c + \epsilon^2 \gamma_2$. The eigenvector $\mathbf{v} = (v_1, v_2)^T$ is normalized so that $\|\mathbf{v}\|_2 = 1$.

The usual expansion leads to the amplitude equations for (Z_1, Z_θ) ,

$$\frac{dZ_1}{dT} = \lambda(\gamma - \gamma_c)Z_1 - [b_0|Z_1|^2 + b_1(\theta)|Z_\theta|^2]Z_1, \quad (3)$$

$$\frac{dZ_\theta}{dT} = \lambda(\gamma - \gamma_c)Z_\theta - [b_1(\theta)|Z_1|^2 + b_0|Z_\theta|^2]Z_\theta. \quad (4)$$

If $\theta = \frac{n\pi}{3}$, $n \in \mathbb{Z}$, the quadratic nonlinearity induces a secular term and the expansion has to include three modes rotated by 120° relative to each other. The parameters can be chosen such that a single solvability condition arises at cubic order [cf. Eq. (5) below, with $Z_{4,5,6} = 0$].

More complex patterns can be described by combining these two analyses. For example, a superhexagon pattern comprised of two hexagon patterns $\{Z_1, Z_2, Z_3\}$ and $\{Z_4, Z_5, Z_6\}$ that are rotated relative to each other by an angle θ_{SH} is described by the amplitude equation

$$\begin{aligned} \frac{dZ_1}{dT} = & \lambda(\gamma - \gamma_c)Z_1 + \sigma \bar{Z}_2 \bar{Z}_3 - [b_0|Z_1|^2 + b_2(|Z_2|^2 + |Z_3|^2)]Z_1 \\ & - \sum_{j=0}^2 b_1 \left(\theta_{SH} + j \frac{2\pi}{3} \right) |Z_{4+j}|^2 Z_1 \end{aligned} \quad (5)$$

and corresponding equations for Z_j , $j=2, \dots, 6$.

The coefficients of the amplitude equations can be written in a simple form, setting $\eta \equiv \eta_r + i\eta_i$:

$$\lambda = \frac{\sqrt{1+\beta^2}}{|\beta|}, \quad \sigma = \frac{2\sqrt{1+\beta^2}(a\eta_r + \eta_i)}{\beta\sqrt{1+a^2}}, \quad (6)$$

$$b_0 = 3\psi + \frac{76}{9}\chi, \quad b_2 = 6\psi + 10\chi + \phi, \quad (7)$$

$$b_1(\theta) = 6\psi + 8f(\theta)\chi, \quad (8)$$

with

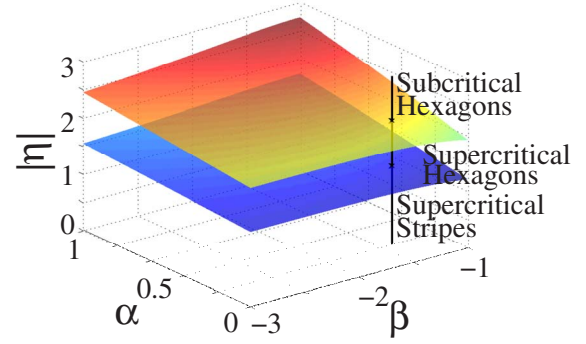


FIG. 2. (Color online) Surfaces $\psi=-2\phi/15$ and $\psi=-\phi/3$ for $\sigma=0$, marking the boundaries of stability between supercritical stripes, supercritical hexagons, and subcritical hexagons, for system parameters α and β with $\mu=-1$ and $\nu=-1$.

$$\psi = 1 - \frac{\alpha}{\beta}, \quad \chi = \frac{-\beta(\nu - \mu\beta)}{2(\mu + \nu\beta)}\sigma^2, \quad (9)$$

$$\phi = -\frac{2(1+\beta^2)}{a\beta(\nu - \mu\beta)} \left(2\sqrt{1+\beta^2}\eta_i^2 - \frac{(a+\beta)\eta_i}{\sqrt{1+a^2}}\sigma \right), \quad (10)$$

$$f(\theta) = \frac{3 + 16 \cos^4 \theta}{(4 \cos^2 \theta - 1)^2}. \quad (11)$$

Here $a = \sqrt{1+\beta^2} + \beta$.

Pattern selection. As shown by Judd and Silber [7] for general two-component reaction-diffusion systems, at the point of degeneracy at which the quadratic coefficient σ vanishes not only stripe patterns but also hexagon or triangle patterns can be stable. The conditions for hexagons (or triangles) to be stable are

$$\phi < 0, \quad -2\phi/15 < \psi < -\phi/3. \quad (12)$$

For $\psi > -2\phi/15$ the bifurcation to hexagons (triangles) is supercritical, while it is subcritical otherwise. For $\psi > -\phi/3$, the hexagons (triangles) are unstable to stripes. Whether hexagon or triangle patterns are stable depends on higher-order terms in the amplitude equations [8], which are not considered here.

Comparing conditions (12) with expressions (9) and (10) shows that over a wide range of the system parameters α and β stripe or hexagon patterns can be made stable by a suitable choice of the forcing function. Specifically, Eq. (10) shows that ϕ is always negative at the degeneracy $\sigma=0$ since $\beta(\nu - \mu\beta) > 0$, which follows from $\mu < 0$ and the condition $k_c^2 > 0$. The surfaces $\psi=-2\phi/15$ and $\psi=-\phi/3$ are shown in Fig. 2 for $\mu=-1$, $\nu=-1$, and $\sigma=0$. These results do not depend qualitatively on the choice of μ and ν as long as $\mu < 0$ and $k_c^2 > 0$. For experiments on the Belousov-Zhabotinsky reaction values for α and β have been reported near the point marked by the vertical line ($\alpha=0.2$, $\beta=-1.4$) [9]. Thus forcing should provide a robust mechanism to induce transitions from stripes to supercritical and subcritical hexagons. A distinguishing feature of these hexagon patterns is that both “up” and “down” hexagons are

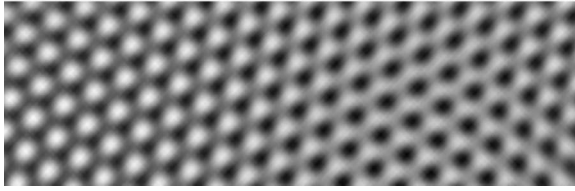


FIG. 3. Competing domains of up- and down-hexagon domains obtained from random initial conditions with linear parameters as in Fig. 1 and nonlinear parameters $\alpha=-1$, $\eta_r=0.4$, and $\eta_i=-0.4(\sqrt{10}+3)$. η_r and η_i chosen so that $\sigma=0$.

simultaneously stable and are likely to form competing domains. Figure 3 shows an example of the competition between “up” and “down” hexagons in a numerical simulation of Eq. (1).

Unfolding the degeneracy, i.e., taking $0 < |\sigma| \ll 1$, the transition to hexagons becomes transcritical and hexagons are stable to stripes for a γ range given by

$$\gamma_c - \frac{\sigma^2}{4\lambda(b_0 + 2b_2)} < \gamma < \gamma_c + \frac{\sigma^2(2b_0 + b_2)}{\lambda(b_2 - b_0)^2} \equiv \gamma_{HS}. \quad (13)$$

Note that $\gamma_{HS} > \gamma_c$, even if Eqs. (12) are not satisfied, since stripes do not exist for $\gamma < \gamma_c$. The instability of hexagons at γ_{HS} only arises if $b_2 > b_0$, that is, if $3\psi + 14\chi/9 + \phi > 0$. With $\sigma \neq 0$ the up-down symmetry of the hexagon amplitude equations is broken and either up or down hexagons are preferred.

Turning to other planforms, Judd and Silber found that rectangular planforms cannot be stable at or near the degeneracy point [7]. Interestingly, however, they find that while superhexagons cannot be stable at the degeneracy point, they can arise in a very small parameter regime in its vicinity if the conditions

$$\phi > 0, \quad -\phi/21 < \psi < \phi/3 \quad (14)$$

are met. They then can be bistable with hexagons. We find that in our system this is not the case within the cubic truncation (5). Equation (10) shows that—for small $|\sigma|$ — ϕ can be made positive only by making η_i small as well [$\eta_i = O(\sigma)$]. Even then ϕ can only be slightly positive, $\phi = O(\sigma)$, requiring that $\psi = O(\sigma)$ in order to satisfy the second condition in Eq. (14). Under these conditions all cubic coefficients in Eqs. (7) and (8) would become of $O(\sigma)$ and without knowledge of the next-order coefficients no stability predictions can be made.

Often weakly nonlinear analysis gives qualitatively useful information beyond its formal regime of validity. We therefore also consider the case $\sigma = O(1)$. Considering superhexagons it should be noted that for $\sigma = O(1)$ the inequalities (14) are not the correct stability conditions, since they were derived assuming $0 < \sigma \ll 1$ and so ignore the angle dependence of the cubic coefficients, which is $O(\sigma)$. We use Eq. (14) therefore only as a guide to locate parameter regimes in which superhexagons may be expected to be stable and then determine the eigenvalues that govern their stability directly from the linearization of Eq. (5) about the equal-amplitude

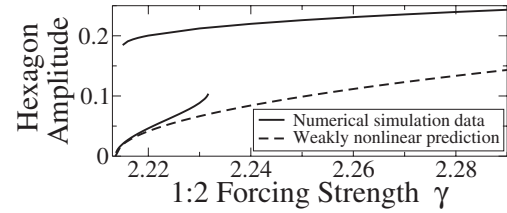


FIG. 4. Numerically obtained hexagon amplitudes for linear parameters as in Fig. 1 and nonlinear parameters $\alpha=0$, $\eta_i=2.38$, and $\eta_r=-2.38/(\sqrt{10}+3)$. η_r and η_i chosen so that $\sigma=0$.

solution $|Z_j| = |Z|$, $j=1, \dots, 6$. One parameter set for which all superhexagon eigenvalues are negative, suggesting that superhexagons are stable, is given by the linear parameters used in Fig. 1 with $\alpha=-1$ and $\eta = \sqrt{2}e^{i\pi/4}$.

Using direct numerical simulations of the forced complex Ginzburg-Landau Eq. (1) we have studied to what extent the predictions of the weakly nonlinear analysis are borne out. In the degenerate case $\sigma=0$, enforced by setting $\eta_i = -a\eta_r$, we find, as predicted, either stripes or hexagons to be stable depending on the values of α and $|\eta|$. To test the stability boundary $\psi = -\phi/3$ in Eq. (12) we vary the 1:3 forcing strength $|\eta|$ with the remaining parameters in Eq. (1) fixed at $\gamma=2.25$ and $\alpha=0$ and the linear parameters as given for Fig. 1 and start the simulations with random initial conditions. The simulations agree with the weakly nonlinear prediction to within 5%. Figure 3 shows a typical hexagonal pattern obtained from random initial conditions exhibiting competing domains of up and down hexagons.

The stability limit $\psi = -2\phi/15$ in Eq. (12) marks the point at which the pitchfork bifurcation to hexagons becomes subcritical. Extracting the cubic coefficient $b_0 + 2b_2$ from transient hexagon patterns (cf. Fig. 5 below) for varying values of $|\eta|$ with all other parameters as well as $\sigma=0$ fixed we find agreement between the weakly nonlinear result and the simulations to within 1%. Figure 4 presents a bifurcation diagram in the supercritical regime but close to the tricritical point (ψ only slightly above $-2\phi/15$). While the weakly nonlinear analysis agrees very well in the immediate vicinity of the bifurcation point, the deviations become significant already for values of γ only 0.5% above γ_c . Most surprisingly, however, as γ is further increased the small-amplitude hexagons undergo a saddle-node bifurcation and in the simulations the solution jumps to large-amplitude hexagons. Both small- and large-amplitude hexagons are simultaneously stable over a range in γ . With increasing $|\eta|$ the saddle-node bifurcation at which the large-amplitude hexagons come into existence is shifted toward smaller values of $\gamma < \gamma_c$. We have not investigated to what extent the existence of the large-amplitude hexagons depends on the parameters α and β of the unforced system.

Away from the degeneracy, $\sigma = O(1)$, the validity of the weakly nonlinear analysis can be severely restricted by the fact that the amplitudes of all stable branches are $O(1)$, which formally suggests the significance of higher-order terms in the expansion. Indeed, in and near the parameter regimes for which the weakly nonlinear analysis predicts stable superhexagon patterns we do not find any indication of

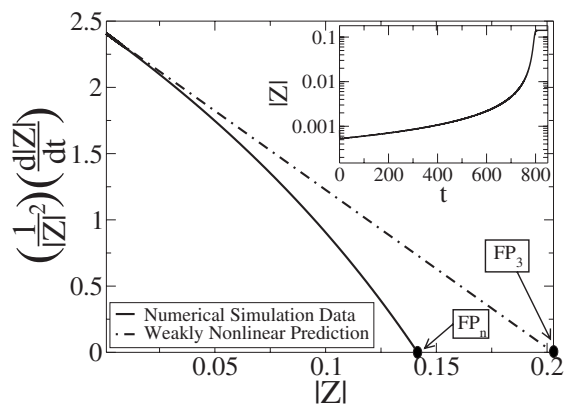


FIG. 5. Extracting the nonlinear coefficients for hexagons from transients (inset) for $\mu=-1$, $\nu=4$, $\beta=3$, $\alpha=-1$, and $\eta=\sqrt{2}e^{i\pi/4}$ (so $\sigma=2.4187$). FP_n corresponds to the fixed point obtained from numerical simulation and FP_3 to that obtained from the weakly nonlinear calculation to cubic order.

their stability. To assess explicitly the significance of the higher-order terms in the amplitude equations for $\sigma=O(1)$ we extract them directly from numerical simulations of transients for the case of hexagon patterns. Figure 5 shows for $\gamma=\gamma_c$ the numerically determined dependence of $|Z|^{-2}d|Z|/dt$ on the hexagon amplitude $|Z|=|Z_j|$, $j=1, 2, 3$. For very small $|Z|$ it agrees well with the weakly nonlinear result $\sigma-(b_0+2b_2)|Z|$, which yields the straight dashed line. However, even for $\gamma=\gamma_c$ the fixed point FP_3 obtained from the hexagon amplitude equations deviates from the numerically obtained fixed point FP_n by 30%. A fit of $|Z|^{-2}d|Z|/dt$ to a higher-order polynomial shows that in the amplitude equation the magnitude of the quartic and quintic terms reach values of 15% and of 20% of the cubic term, respectively. This supports our interpretation that in this regime the cubic amplitude equation does not allow quantitative predictions.

In summary, we have investigated the regular spatial planforms that can be stably excited in a system undergoing a Hopf bifurcation by applying a periodic forcing function that resonates with the second and third harmonic of the Hopf frequency. We have done so within the weakly nonlinear

regime by deriving from the complex Ginzburg-Landau Eq. (1) the appropriate amplitude equations describing the selection between various planforms. By tuning the phase of the forcing close to $3\omega_h$ one can always reach the point of degeneracy at which no quadratic terms arise in the amplitude equations, despite the quadratic interaction in the underlying complex Ginzburg-Landau equation. Over a wide range of the parameters of the unforced system, hexagon or stripe patterns can be stabilized depending on the forcing function. In the former case competing domains of up and down hexagons are found in numerical simulations when starting from random initial conditions. Hexagons can arise from either a supercritical or subcritical pitchfork bifurcation, which we have shown analytically and confirmed numerically. Moreover, numerical simulations have shown the existence of hexagons with much larger amplitude, which can be bistable with the supercritical hexagons.

Surprisingly, despite the extensive control afforded by the two forcing terms, no square, rectangle, or superhexagon patterns are stable in the vicinity of the degeneracy $\sigma=0$, irrespective of the parameters of the unforced system. While in the regime in which hexagons arise in a strongly transcritical bifurcation the weakly nonlinear theory suggests the possibility of stable superhexagons, direct numerical simulations of the complex Ginzburg-Landau equation indicate no such stability and we show that terms of higher order in the amplitudes are relevant.

By introducing a further forcing frequency, which is also close to the 2:1-resonance, the transcritical bifurcation to hexagons can be avoided. As we show in a separate paper, the corresponding, more elaborate weakly nonlinear theory correctly predicts stable quasipatterns comprised of four, five, or more modes [10].

For stronger forcing the spatially periodic standing waves interact with a spatially homogeneous oscillation that is also excited by the forcing. The interaction between these two modes could lead to interesting patterns, which are, however, beyond the scope of this paper.

We gratefully acknowledge support by NSF through Grants No. DMS-0309657 and No. DMS-0309657.

-
- [1] B. Christiansen, P. Alstrom, and M. T. Levinsen, *Phys. Rev. Lett.* **68**, 2157 (1992); W. S. Edwards and S. Fauve, *Phys. Rev. E* **47**, R788 (1993); A. Kudrolli, B. Pier, and J. Gollub, *Physica D* **123**, 99 (1998); H. Arbell and J. Fineberg, *Phys. Rev. E* **65**, 036224 (2002).
- [2] W. Zhang and J. Vinals, *Phys. Rev. E* **53**, R4283 (1996); M. Silber, C. M. Topaz, and A. C. Skeldon, *Physica D* **143**, 205 (2000); A. M. Rucklidge and M. Silber, *Phys. Rev. E* **75**, 055203(R) (2007).
- [3] A qualitative effect on the system may also be produced through differences in the forcing frequencies [cf. C. Topaz, J. Porter, and M. Silber, *Phys. Rev. E* **70**, 066206 (2004)].
- [4] P. Couillet and K. Emilsson, *Physica D* **61**, 119 (1992).
- [5] J. Conway and H. Riecke (unpublished).
- [6] P. Couillet, T. Frisch, and G. Sonnino, *Phys. Rev. E* **49**, 2087 (1994).
- [7] S. L. Judd and M. Silber, *Physica D* **136**, 45 (2000).
- [8] M. Silber and M. R. E. Proctor, *Phys. Rev. Lett.* **81**, 2450 (1998).
- [9] F. Hynne and P. Graae Sørensen, *Phys. Rev. E* **48**, 4106 (1993).
- [10] J. Conway and H. Riecke, *Phys. Rev. Lett.* (to be published).